

**Supplemental Information**

**MALT1 Phosphorylation Controls**

**Activation of T Lymphocytes**

**and Survival of ABC-DLBCL Tumor Cells**

**Torben Gehring, Tabea Erdmann, Marco Rahm, Carina Graß, Andrew Flatley, Thomas J. O'Neill, Simone Woods, Isabel Meininger, Ozge Karayel, Kerstin Kutzner, Michael Grau, Hisaaki Shinohara, Katja Lammens, Regina Feederle, Stefanie M. Hauck, Georg Lenz, and Daniel Krappmann**

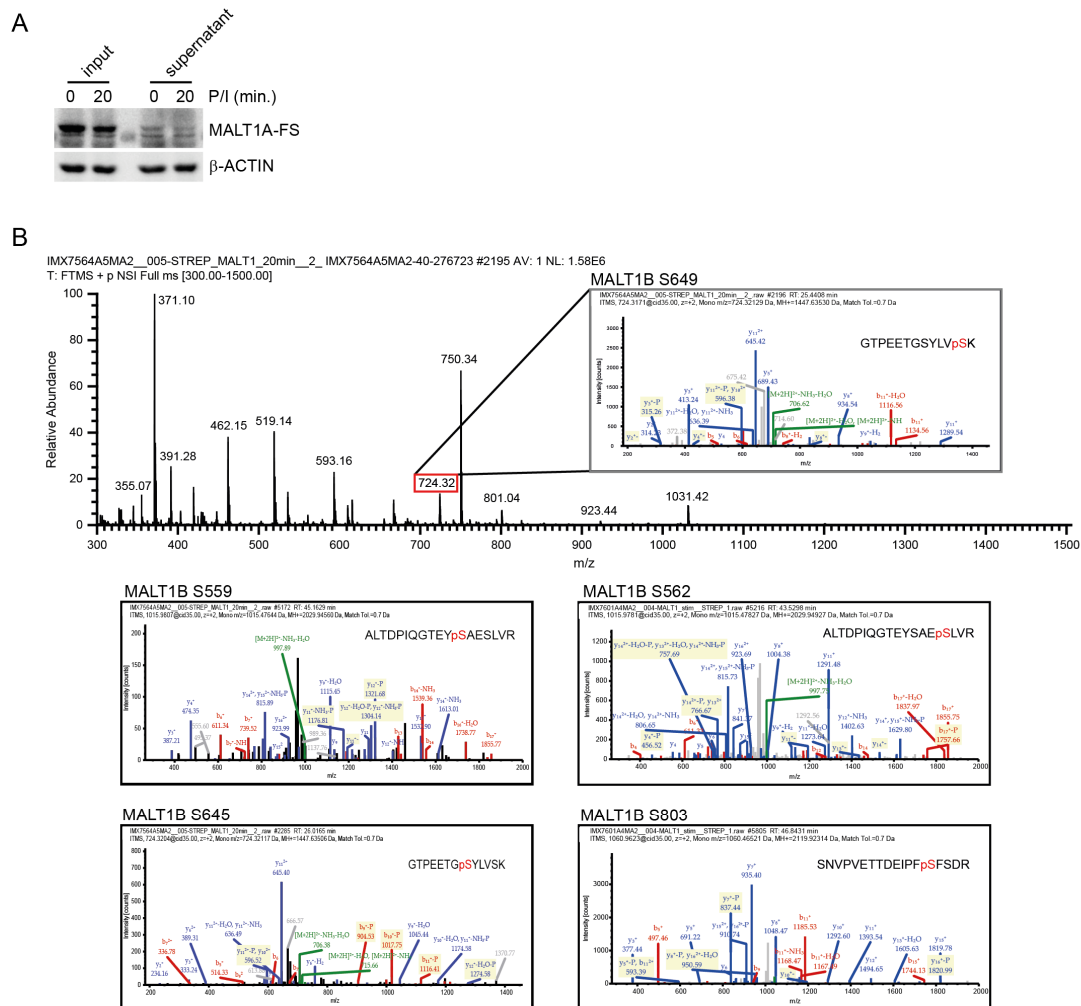


**Figure S1: Identification of C-terminal MALT1 phosphorylation sites. Related to Figure 1.**

A) Efficient enrichment of MALT1 from extracts using ST-PD for LC-MS/MS analysis. Protein level of MALT1A-FS before (input) and after (supernatant) ST-PD is shown.

B) MS1 spectrum for MALT1 phosphorylation site S649 with corresponding MS2 spectrum. For the other identified sites, only the MS2 spectra are shown.

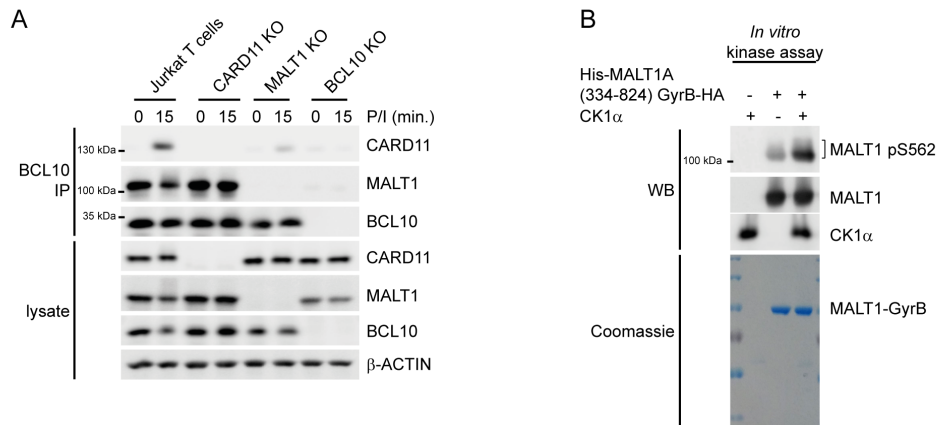
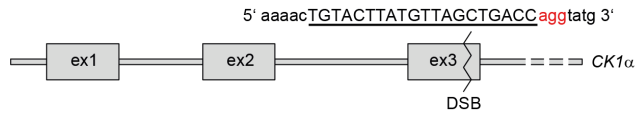


**Figure S2: Lack of CBM complex assembly in CARD11, MALT1 or BCL10 KO Jurkat T cells. Related to Figure 3.**

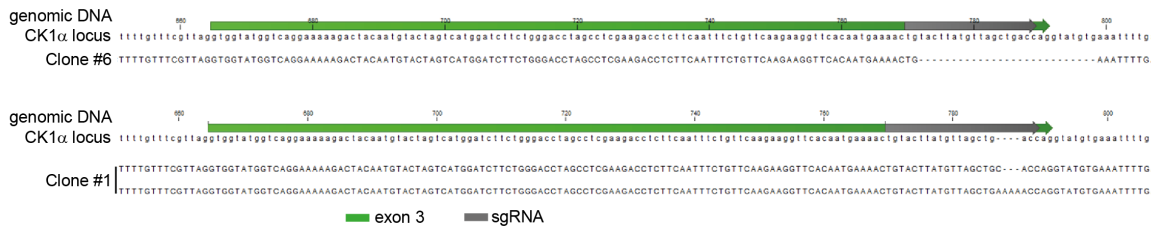
A) CBM complex formation in parental Jurkat T cells and CARD11, MALT1 or BCL10 KO Jurkat T cells was determined by BCL10-IP and WB following P/I stimulation.

B) *In vitro* protein kinase assay using baculovirally-produced 6xHis-MALT1-GyrB-HA (aa 334-813) as a substrate for CK1 $\alpha$  was performed and analyzed by Western Blot using the phospho-specific antibody against MALT1B S562.

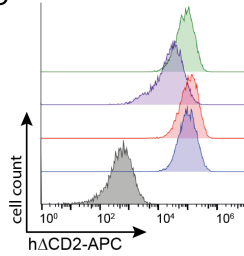
A



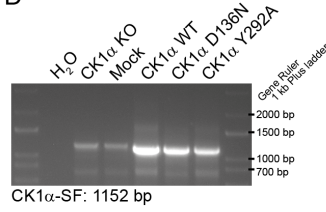
B



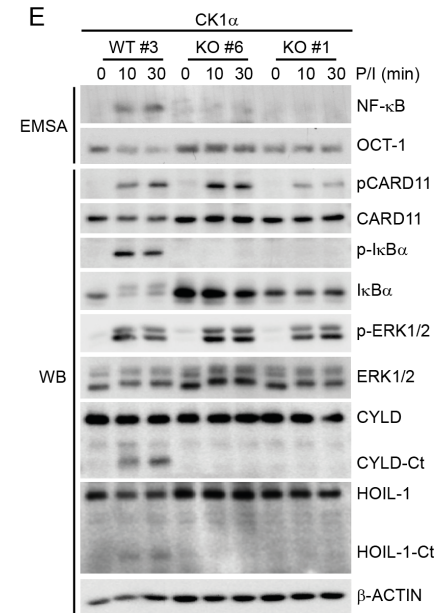
C



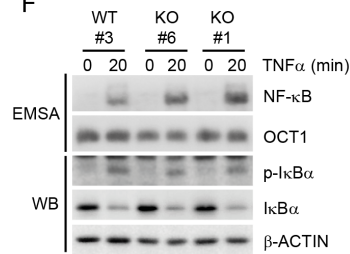
D



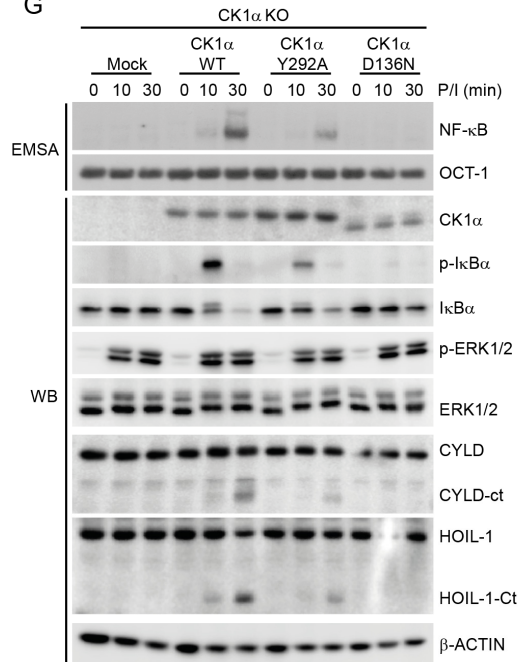
E



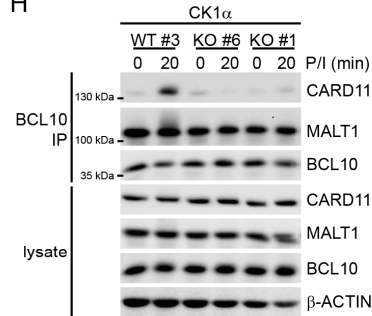
F



G



H



I

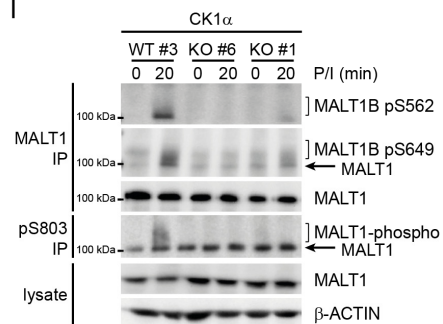


**Figure S3: Generation of CK1 $\alpha$ -deficient Jurkat T cells. Related to Figure 4.**

A) Scheme of CK1 $\alpha$  genomic locus. Exon 3 of CK1 $\alpha$  was targeted using the CRISPR/Cas9 system with a sgRNA sequence as depicted. Adjacent PAM site is highlighted in red.

B) Summary of sequencing of the genomic DNA locus surrounding exon 3 in two independent CK1 $\alpha$ -deficient Jurkat T cell clones. CRISPR Cas9 led to a homozygous deletion (clone #6) or a heterozygous deletion and insertion (clone #1), which always result in a frameshift and premature stop codons.

C) CK1 $\alpha$ -deficient Jurkat T cells were reconstituted with CK1 $\alpha$  WT, a kinase-dead version (D136N), and a CARD11-binding mutant (Y292A). Levels of co-expressed surface marker h $\Delta$ CD2 protein were determined by FACS.

D) mRNA of CK1 $\alpha$  variants was isolated from infected cells and correct size of mRNA was analyzed by amplifying the cDNAs using specific ST-tag PCR primer. By sequencing expression of the correct full length CK1 $\alpha$  mRNA and the presence of respective mutations was verified (data not shown).

E) NF- $\kappa$ B signaling and MALT1 substrate cleavage in CK1 $\alpha$ -deficient Jurkat T cells in response to P/I stimulation was analyzed by EMSA and WB.

F) TNF $\alpha$  stimulation of CK1 $\alpha$ -deficient cells. NF- $\kappa$ B signaling was analyzed by I $\kappa$ B $\alpha$  phosphorylation/degradation and NF- $\kappa$ B DNA binding in WB and EMSA, respectively.

G) Effects of CK1 $\alpha$  kinase-dead and CARD11-binding mutant on NF- $\kappa$ B signaling, and MALT1 substrate cleavage after P/I stimulation were assessed by EMSA and WB. MAPK pathway activation was analyzed by Western blotting.

H) CBM complex assembly was determined in parental and CK1 $\alpha$ -deficient Jurkat T cells after P/I stimulation using BCL10-IP and WB.

I) Phosphorylation of MALT1 at S562, S649 and S803 in parental and CK1 $\alpha$ -deficient Jurkat T cells after P/I stimulation using MALT1-IP and WB.

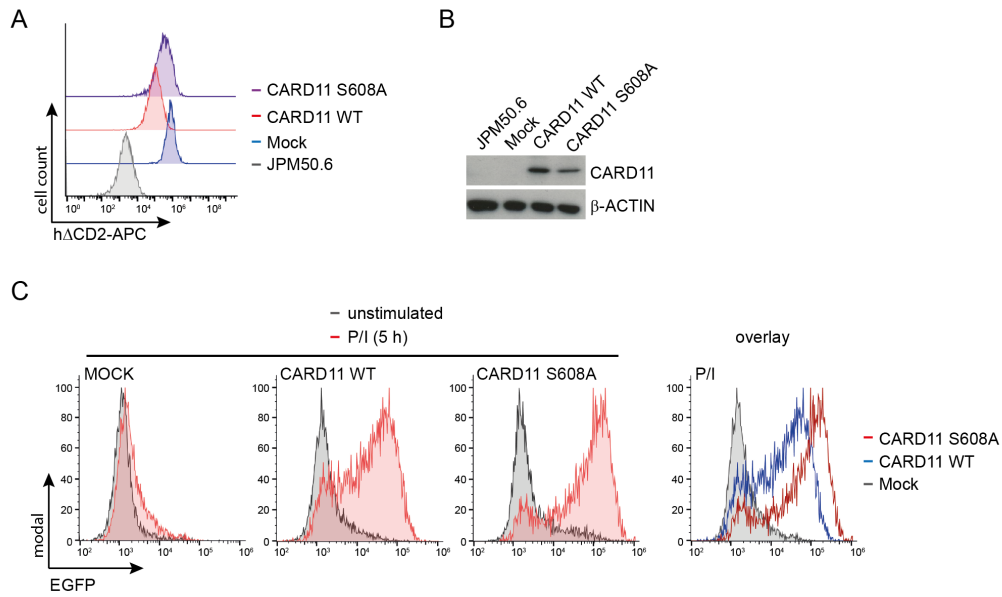


**Figure S4: Lentiviral reconstitution of CARD11-deficient JPM50.6 T cells. Related to Figure 4.**

A) CARD11-deficient JPM50.6 cells were transduced with CARD11 WT and CARD11 S608A lentiviruses and equivalent transduction was determined by FACS analyses of co-expressed surface marker hΔCD2.

B) CARD11 WT and S608A protein expression was analyzed by WB.

C) Mock, CARD11 WT and CARD11 S608A expressing CARD11-deficient JPM50.6 containing an EGFP NF-κB reporter were stimulated with P/I for 5h. Expression of EGFP was analyzed by FACS. Right panel shows the overlay of EGFP expression in mock, CARD11 WT and CARD11 S608A reconstituted cells after P/I stimulation.

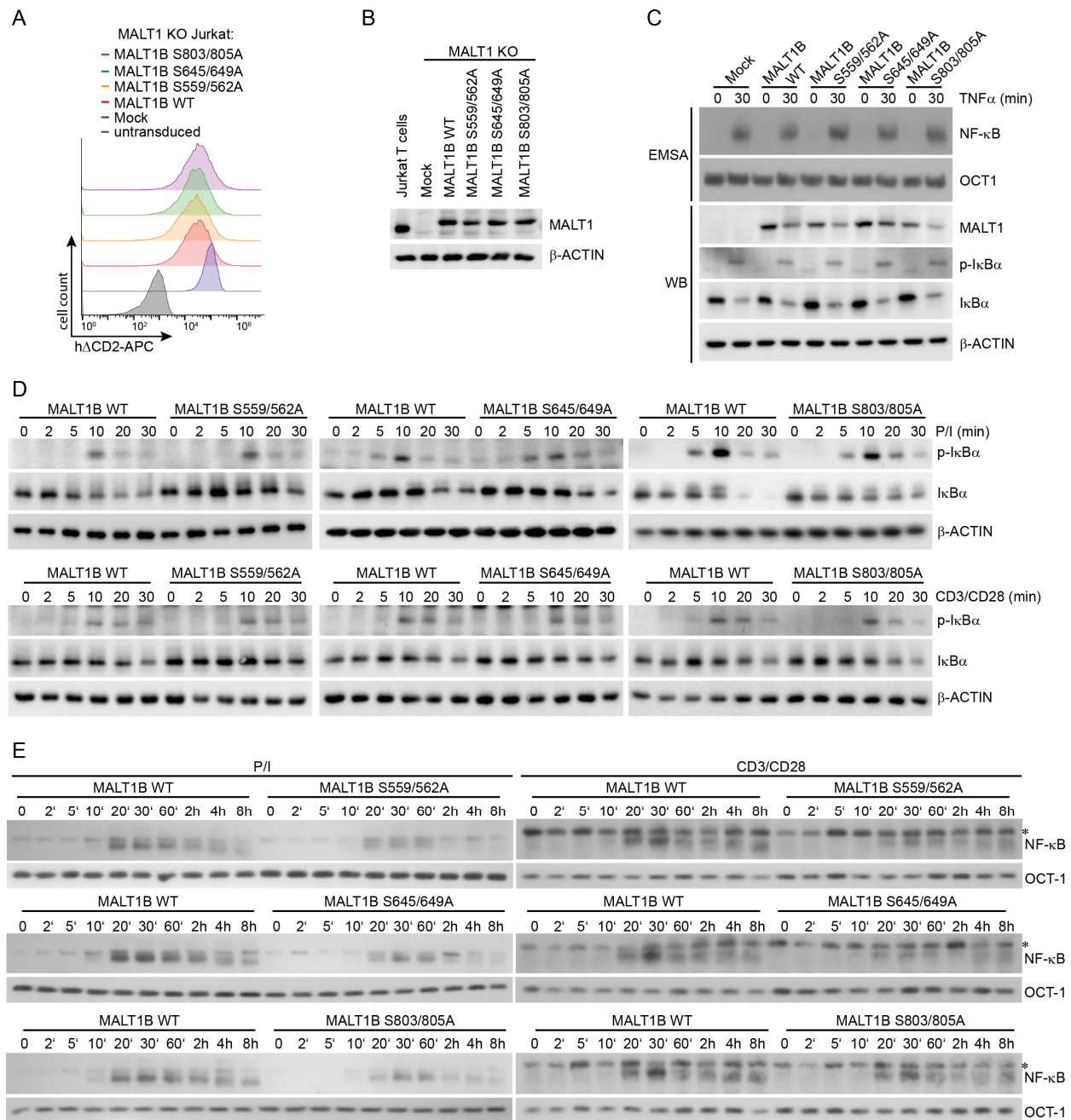


**Figure S5: Pairwise mutations of MALT1 phospho-sites impairs TCR/CD28 and P/I-induced NF- $\kappa$ B signaling in Jurkat T cells. Related to Figure 5.**

A) Transduction efficiency of MALT1 KO Jurkat T cells with MALT1B WT or phospho-defective S/A mutants was monitored by expression of surface marker hA2CD2 in FACS.

B) Expression MALT1B WT and mutants was assessed by WB.

C) TNF $\alpha$  stimulation of MALT1-deficient Jurkat T cells reconstituted with MALT1B WT or phospho-defective S/A mutants. NF- $\kappa$ B activation was determined in EMSA and WB.

D) Effects of MALT1B S/A mutants on I $\kappa$ B $\alpha$  phosphorylation and degradation after P/I or CD3/CD28 stimulation were investigated by WB.

E) Effects of MALT1B S/A mutants on NF- $\kappa$ B activation after P/I or CD3/CD28 stimulation were investigated by EMSA. Unspecific bands are marked with asterisk.



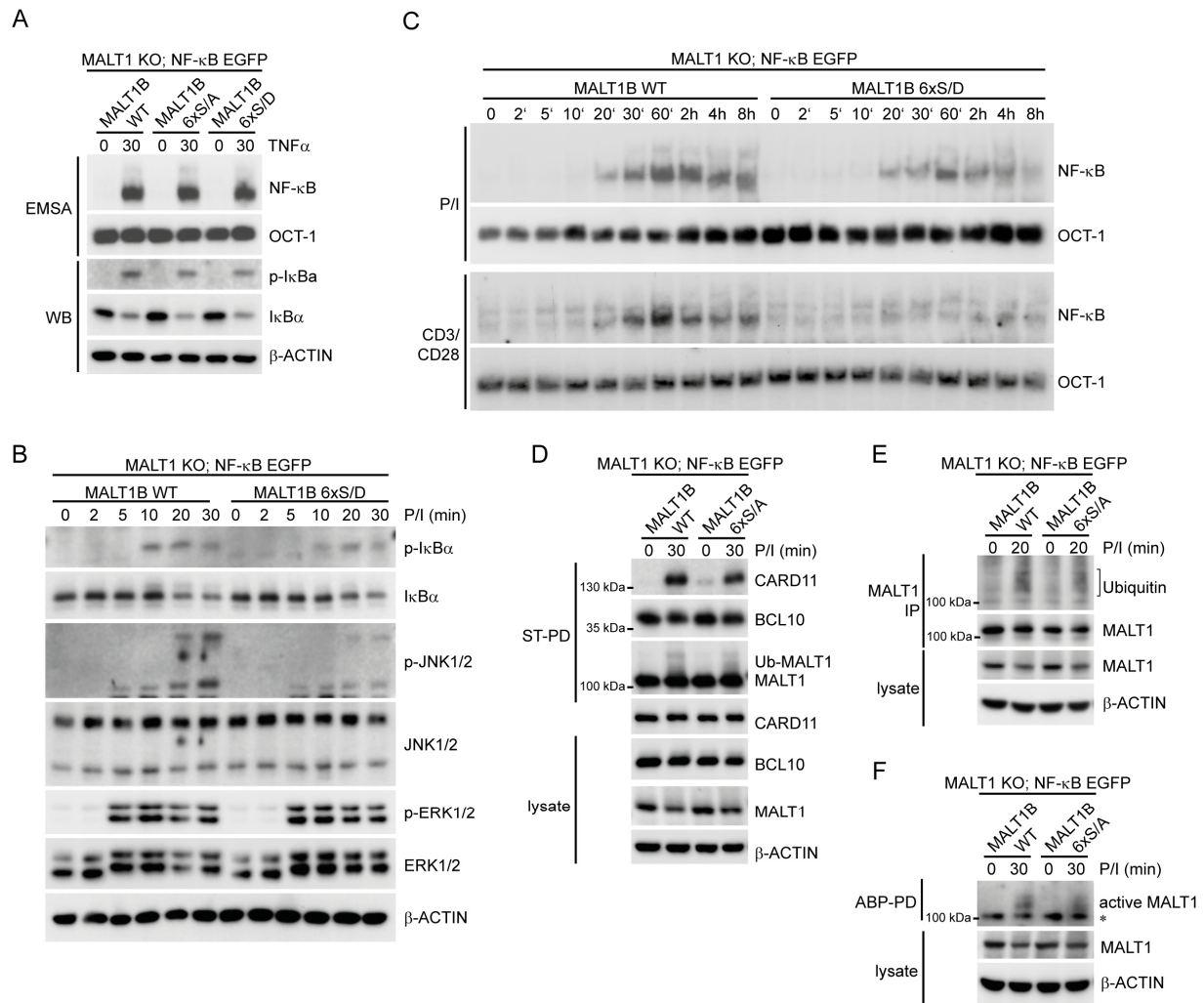


**Figure S6: C-terminal MALT1 phosphorylation is required for efficient NF-κB activation in Jurkat T cells.**

**Related to Figure 5.**

A) TNFα stimulation of MALT1-deficient Jurkat T cells reconstituted with MALT1B WT, 6xS/A and 6xS/D.

NF-κB activation was determined in EMSA and WB.

B) MALT1-deficient Jurkat T cells reconstituted with MALT1B WT and combinatory 6xS/D mutant were stimulated with P/I and their effects on IκBα phosphorylation and degradation as well as JNK and ERK activation were investigated by WB.

C) MALT1-deficient Jurkat T cells reconstituted with MALT1B WT and combinatory 6xS/D mutant were stimulated with P/I or CD3/CD28 and their NF-κB DNA binding were determined by EMSA.

D) Recruitment of MALT1-SF constructs to CARD11 is not effected by MALT1B 6xS/A mutant after P/I stimulation monitored by WB after ST-PD.

E) MALT1-deficient Jurkat T cells reconstituted with MALT1B WT and combinatory 6xS/A mutant were stimulated with P/I. Effects on MALT1 ubiquitination after P/I stimulation were detected by WB after MALT1-IP.

F) MALT1 protease activation of MALT1B WT and MALT1 B 6xS/A after P/I stimulation was analyzed using Streptavidin-PD of active MALT1 after coupling to an activity-based probe (ABP). Active MALT1 is modified and the asterisk indicates the migration of a cross-reaction of the Streptavidin-PD with Strep-Tagged MALT1.

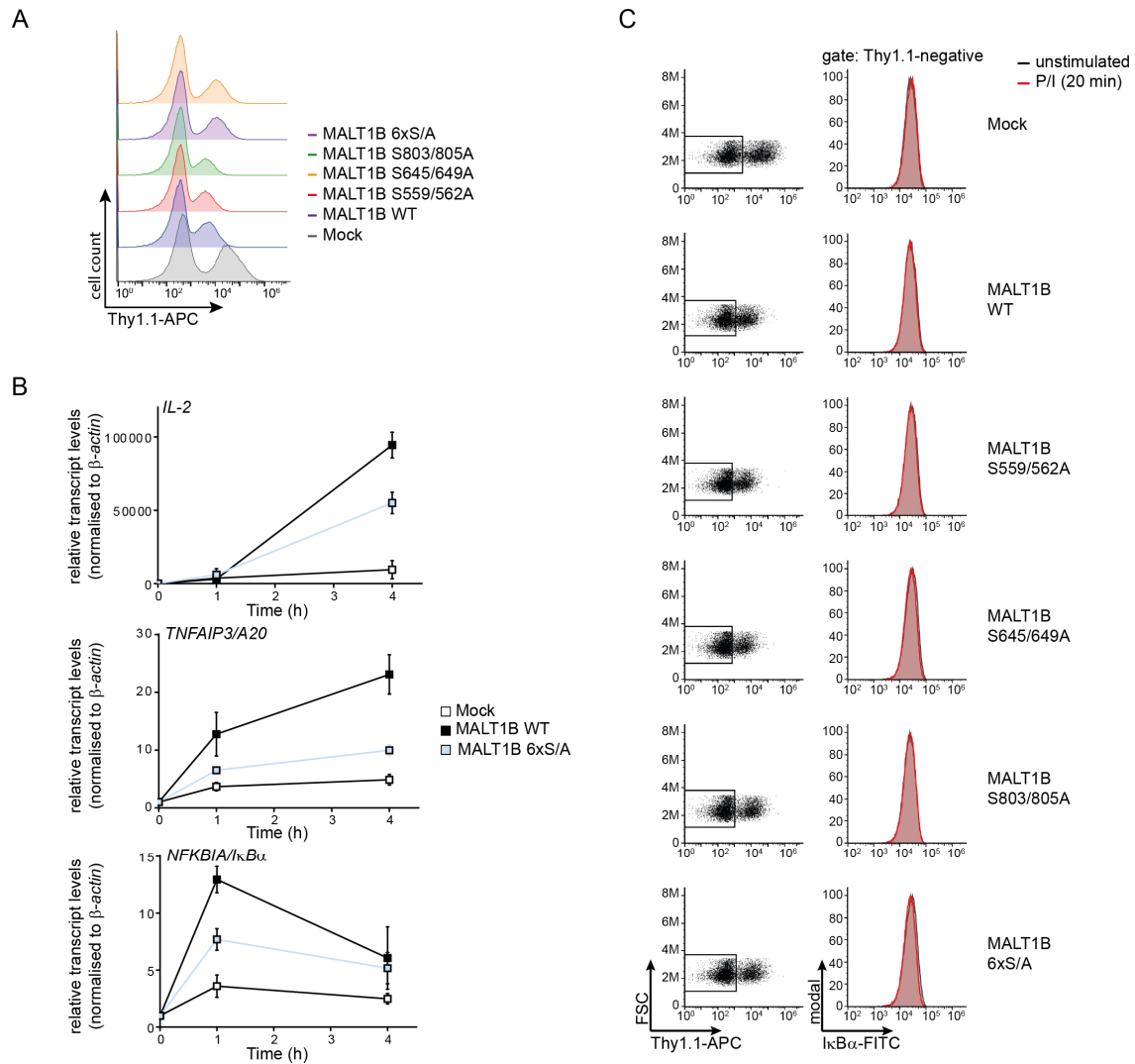


**Figure S7: Analyses of retroviral reconstitutions of primary mCD4 T cells with MALT1 WT and S/A mutants. Related to Figure 6.**

A) Transduction efficiency of murine CD4 T cells from MALT1<sup>-/-</sup> mice was monitored by the surface marker Thy1.1 in FACS.

B) mRNA induction of NF- $\kappa$ B target genes (*IL-2*, *TNFAIP3/A20* and *NFKBIA/IkB $\alpha$* ) analyzed by qRT-PCR in MALT1 KO CD4 T cells reconstituted with MALT1B WT or phospho-defective 6x S/A mutant after 1h or 4h of CD3/CD28 stimulation. Transcript levels were normalized to mRNA levels of  $\beta$ -actin. The data represent the mean  $\pm$  SD of 4 biological replicates.

C) Retroviral MALT1 constructs also carry a Thy1.1 surface marker linked by an IRES sequence. Uninfected Thy1.1-negative cells were analyzed for I $\kappa$ B $\alpha$  degradation after P/I stimulation by FACS, showing that I $\kappa$ B $\alpha$  degradation relies on successful expression of MALT1.